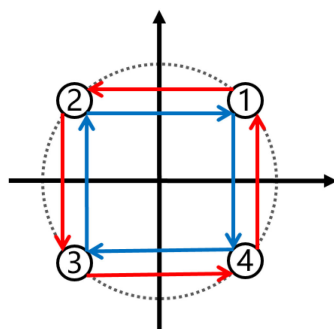


QPSK Training Sequence-Based Both OSNR and Chromatic Dispersion Monitoring in DWDM Systems

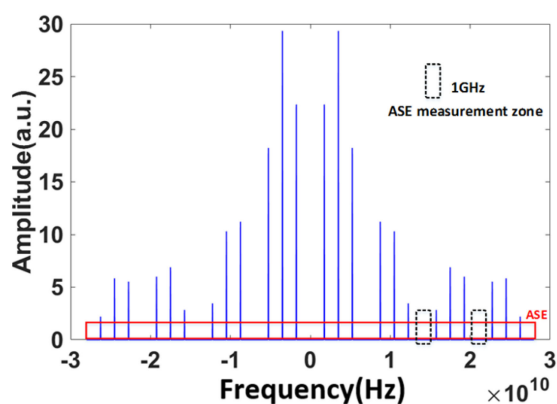
Volume 10, Number 4, August 2018

Feilong Wu
Aiyang Yang
Peng Guo
Yaojun Qiao
Lingwei Zhuang
Shaojian Guo



11223344-11443322

(a)



(b)

DOI: 10.1109/JPHOT.2018.2859428

1943-0655 © 2018 IEEE

QPSK Training Sequence-Based Both OSNR and Chromatic Dispersion Monitoring in DWDM Systems

Feilong Wu¹,¹ Aiying Yang,¹ Peng Guo¹,¹ Yaojun Qiao¹,²
Lingwei Zhuang,² and Shaojian Guo²

¹School of Optics and Photonics, Beijing Institute of Technology, Beijing 100081, China

²State Key Laboratory of Information Photonics and Optical Communications, School of Information and Communication Engineering, Beijing University of Posts and Telecommunications, Beijing 100876, China

DOI:10.1109/JPHOT.2018.2859428

1943-0655 © 2018 IEEE. Translations and content mining are permitted for academic research only.

Personal use is also permitted, but republication/redistribution requires IEEE permission.

See http://www.ieee.org/publications_standards/publications/rights/index.html for more information.

Manuscript received June 3, 2018; revised July 20, 2018; accepted July 21, 2018. Date of publication August 2, 2018; date of current version August 10, 2018. This work was supported in part by National Natural Science Foundation of China under Grant 61427813 and Grant 61331010, and in part by the State Key Laboratory of Advanced Optical Communication Systems and Networks, China. Corresponding authors: Aiying Yang and Peng Guo (e-mail: guopeng0304@bit.edu.cn; yangaiying@bit.edu.cn).

Abstract: We design a quadrature phase-shift keying training sequence (QPSK-TS) for monitoring both optical signal-to-noise ratio (OSNR) and chromatic dispersion (CD) in a dense wavelength division multiplexing (DWDM) system. By applying fast Fourier transform on the QPSK-TS, a comb-like spectrum with discrete peaks can be obtained. OSNR can be calculated by measuring the power of the amplified spontaneous emission (ASE) noise in the gaps between these peaks. Moreover, we search the optimal order in the fractional domain to calculate the CD after applying fractional Fourier transform on the QPSK-TS signal. The proposed method shows large ASE noise and optical nonlinearity tolerance in simulation results (<1.0 dB error within 24 dB after transmission over 1000 km with 3 dBm per channel launch power, and <90 ps/nm error within 33400 ps/nm). Furthermore, the experimental results demonstrate high accuracy of the proposed method (≤ 1.0 dB error within 28 dB and <40 ps/nm error within 1670 ps/nm after 100 km single channel transmission).

Index Terms: Training sequence, fractional domain, fiber optics systems.

1. Introduction

OSNR and CD are two important factors affecting the quality of optical network communications [1], [2]. Several OSNR measurement methods have been proposed [3]–[6]. In [4], [5], the method of measuring OSNR in the frequency domain based on the QPSK training sequence and the 16-QAM training sequence was proposed and experimentally demonstrated, which has high accuracy in measuring OSNR as ASE noise can be separated from other nonlinear noise. A method based on linear-frequency modulation (LFM) signal measuring OSNR is proposed recently [6]. Accurate measurement of CD is critical for evaluating system performance and subsequent signal processing [7]. The current state of the art of performance monitoring indicates that there is a decreased interest in how to monitor CD, since as mentioned in [8], coherent receivers can compensate up to 100000 ps/nm of CD. However from an academic point of view the interest still remains due to the expected increase in the dynamic behavior of optical networks in order to improve efficiency. There

have been reported CD estimation or monitoring techniques by taking training sequence or LFM signal as a pilot [9]–[12]. The method of blind CD estimation based on FrFT has been proved to be feasible by simulation and experiment [8], [13]. However, the mentioned measurement methods above are only capable of measuring one of OSNR and CD, which cannot meet our requirement when we have only one type of data samples for measuring OSNR or CD.

In this paper, we design a QPSK-TS for monitoring both OSNR and CD in DWDM systems. The QPSK-TS has periodic phase shifting and the spectrum of the QPSK-TS is a comb-like spectrum with different frequency components. The peaks of the comb-like spectrum are discrete. The power of the ASE noise in the gaps between these peaks is measured to calculate the OSNR. On the other hand, after applying FrFT on the QPSK-TS, the energy concentration of the QPSK-TS signal corresponding to different orders is different in the fractional domain. By searching for the optimum order of the signal, the accumulated CD can be obtained. With the QPSK-TS design, it is allowed to calculate both OSNR and CD from the same set of data samples, which will reduce the sampling data types and save our sampling time. The QPSK-TS can also be used as a time domain pilot as done in [4] if needed. In this paper, we focus on the design of the QPSK-TS and the performance of monitoring OSNR and CD. In our simulation, we analyze the NL tolerance of the method when OSNR is monitored in a 28 Gbaud QPSK system. The ASE noise tolerance and NL tolerance are explored while monitoring CD in the simulation. At the end of the paper, we conduct an experiment with 20 GBaud 100 km single-channel optical fiber transmission based on our proposed method.

2. Monitoring Principle

2.1 QPSK-TS Designing Principle

The general QPSK signal can be expressed as:

$$x(t) = A \cos(\omega t + \theta) \quad (1)$$

where A is the amplitude, ω is the signal angular frequency, and θ is the initial phase.

From [4], we can use a QPSK training sequence with one single spectrum component as a time pilot, and then the ASE noise power can be measured by the spectrum components different from dedicated pilot frequencies, so that we can calculate OSNR. However, due to the single-frequency property of the training sequence, we cannot obtain optimum order which is used to calculate CD after FrFT. Using the FrFT method to measure CD requires that the signal has many spectral components, such as QPSK signal [8] and LFM signal [12]. For us, we try to measure the CD while ensuring the measurability of OSNR. And the training sequence we designed can meet this requirement very well.

As shown in Fig. 1(a), the QPSK-TS we designed is generated by controlling the phase of QPSK signals for periodic migration. The phase shift first rotates anticlockwise in the first quadrant. The phase migration trajectory in the quadrant can be expressed as 11223344–11443322, where the number represents the I/Q coordinates of the quadrant. Its corresponding spectrum is shown in Fig. 1(b). This is a comb-like spectrum with different frequency components, whose peaks are discretely arranged cyclically and symmetrical about the center frequency of the signal. The period of QPSK-TS is 16 symbols, so that the peak component is at an integer multiple of $\pm R_s/16$, where R_s is the baud rate. How to use the QPSK-TS to calculate OSNR and CD will be detailed in the next two subsections.

2.2 OSNR Monitoring Principle

OSNR can be calculated according to the following definition [6]:

$$OSNR = 10 \times \lg \left[\frac{(P_{Total} - P_{ASE}) B_{AM}}{N_{AM} B_R} \right] \quad (2)$$

$$P_{ASE} = B_{Sample} N_{AM} / B_{AM} \quad (3)$$

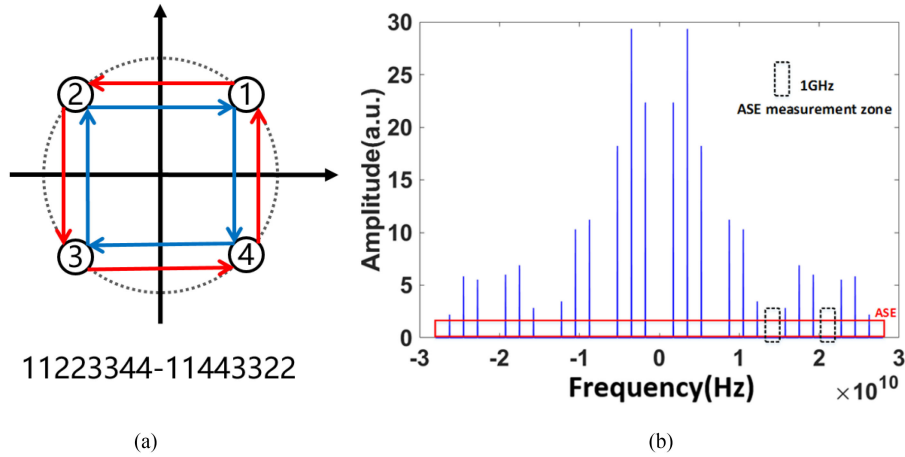


Fig. 1. (a) QPSK-TS phase shift trajectory. (b) QPSK-TS comb-like spectrum and ASE noise distribution.

where P_{Total} is the total power of the received signal, P_{ASE} is the total power of ASE noise in the received signal, N_{AM} is the power of noise in ASE measurement zone as shown in Fig. 1(b), B_{AM} is the bandwidth of ASE measurement zone and B_R is the standard OSNR measurement bandwidth (12.5 GHz), B_{Sample} is the bandwidth of the sampled signal.

As shown in Fig. 1(b), in the linear transmission model, the spectrum consists of the QPSK-TS's spectral components and a flat pedestal which is ASE noise. We measure the power of the ASE noise in these gaps to separate the ASE noise from the received signal and then calculate the OSNR. In addition, the nonlinear phase noise appears around the peaks of the spectrum and the large power peak suffers more nonlinear phase noise than the smaller one [4], [5]. Therefore, we select the gap with low peak and large spacing in the edge of the spectrum for ASE noise measurement to reduce the influence of nonlinearity on ASE noise measurement.

2.3 CD Monitoring Principle

Corresponding to different orders of FrFT, the signal has a different degree of energy aggregation. The signal's highest degree of energy concentration corresponds to the optimum order (p_{opt}) after FrFT. For the same signal, different accumulated CD correspond to different p_{opt} . Therefore, we can calculate the accumulated CD of the received signal by searching the p_{opt} after FrFT.

The FrFT is defined with the help of the transformation kernel K_α as [14], [15]:

$$K_\alpha(u, t) = \begin{cases} A_\alpha \exp \left[j \left(\frac{1}{2} u^2 \cot \alpha - ut \csc \alpha + \frac{1}{2} t^2 \cot \alpha \right) \right], & \alpha \neq n\pi \\ \delta(u - t), & \alpha = 2n\pi \\ \delta(u + t), & \alpha = (2n \pm 1)\pi \end{cases} \quad (4)$$

with

$$\begin{cases} A_\alpha = \sqrt{\frac{1 - j \cot \alpha}{2\pi}} \\ \alpha = p\pi/2, p \neq 2n \end{cases} \quad (5)$$

where n is the integer, α is the rotation angle, p is the order of FrFT.

The FrFT of $x(t)$ is defined using the kernel and denoted by $X_\alpha(u)$:

$$X_\alpha(u) = \int_{-\infty}^{+\infty} K_\alpha(u, t) x(t) dt \quad (6)$$

According to the energy conservation law, the optimum order of FrFT can be calculated by a statistical parameter $EC(p)$ which can be used to describe the energy concentration of the signal

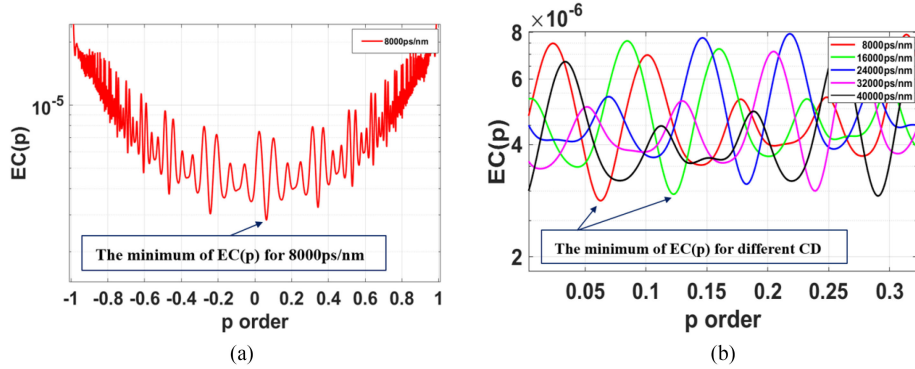


Fig. 2. (a) $EC(p)$ vs p orders for QPSK-TS with a specific CD. (b) $EC(p)$ vs p orders for QPSK-TS with different CD.

in different order p [16]:

$$EC(p) = \int_{-\infty}^{+\infty} |X_p(u)|^4 du \quad (7)$$

where $X_p(u)$ is the p order of FrFT of the signal $x(t)$ and the fourth power in the formula is to make the energy concentration effect more obvious. For QPSK signal, we can get the p_{opt} of FrFT by searching the minimum of $EC(p)$.

The p_{opt} of the signal $x(t)$ has the following relation with the accumulated CD [13]:

$$DL = \frac{2\pi c}{\lambda^2} \cot \left[(p_{opt} - 1) \frac{\pi}{2} \right] \frac{dt}{d\omega} \quad (8)$$

where D is the dispersion coefficient of the fiber, L is the transmission fiber length, c is the vacuum speed of light, λ is the carrier wavelength, and p_{opt} is the optimal order after FrFT of $x(t)$. Thus, we can calculate the CD when the p_{opt} of the QPSK-TS signal is obtained.

Taking QPSK-TS signal with a specific CD as an example. We first apply FrFT with different order on the received signal, and then scan the orders by a step size of $\Delta p = 0.001$, so we can get a $EC(p)$ - p plot, as shown in Fig. 2(a). The minimum of $EC(p)$ corresponds to the p_{opt} . As shown in Fig. 2(b), the p_{opt} increases with an increase in the accumulated CD.

Notice that there must be estimation error caused by the step size which can be expressed as:

$$|\Delta p_{est}| = |p_{opt-est} - p_{opt-ref}| \quad (9)$$

where $p_{opt-est}$ is the estimated optimum order by scanning, $p_{opt-ref}$ is the reference optimum order corresponding to the reference CD. When $0 \leq |\Delta p| < 0.001$, the resulting CD estimation error is considered acceptable. We can improve the accuracy of the measurement by reducing the step size Δp , but it will increase the computational complexity accordingly. In addition, we can use the method in [16] to search the optimum order by dividing the search process into coarse stage with fewer samples and fine stage with more samples, which will reduce computational complexity when we need higher measurement accuracy.

2.4 System Setup and Parameter Setting

To evaluate our method for simultaneously monitoring OSNR and CD, the system set up using commercial software Virtual Photonics Inc. (VPI) is shown in Fig. 3. We set up a maximum of 5 channels with 50 GHz channel spacing, and the middle channel is QPSK-TS signal, while the other four channels transmit the standard QPSK signal. The center frequency of the laser is set to 193.1 THz and the laser linewidth is 300 kHz. The symbol rates of all signals are both 28 GBaud. The signals transmit over single-mode fiber (SMF) link after multiplexed. The SMF link with chromatic

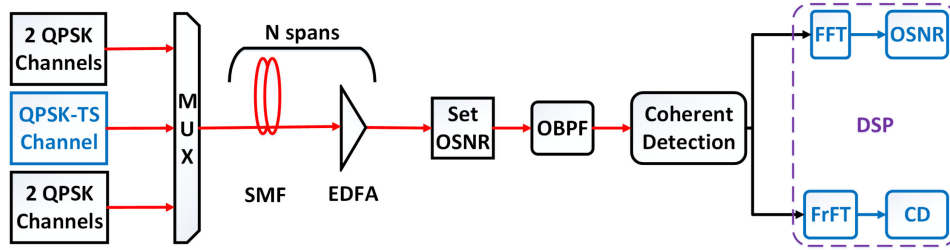


Fig. 3. Schematic diagram of simultaneously monitoring OSNR and CD.

dispersion coefficient 16.7 ps/nm/km, fiber loss 0.2 dB/km and each span 100 km are used in our system. The nonlinear coefficient is set to 2.6×10^{-20} m²/W when we need to consider the nonlinear noise. The erbium-doped optical fiber amplifier (EDFA) in each span amplifies the power of the signal with a fixed power, completely compensating for the energy loss caused by the fiber link. At the end of the link, we use the Set OSNR module to control the ASE noise of the transmission. The QPSK-TS signal is received coherently after an optical band-pass filter (OBPF), whose bandwidth is set to 50 GHz. We use the digital signal processing (DSP) method to process the coherently received signal data off-line. The OSNR in band is calculated by measuring the power of the ASE noise in the frequency domain. On the other hand, we calculate the CD in the fractional domain. The sampling rate is 56 GSa/s and the total number of the sampled data is only 2048 for OSNR and CD monitoring in simulation. For each simulation condition, there are 20 frames for calculating the mean, maximum, minimum, and standard deviation of the OSNR and CD measurements.

3. OSNR Monitoring Simulation Results

The ASE noise power with a bandwidth zone of 1 GHz is measured to calculate the OSNR, as shown in Fig. 1(b), and the OSNR range is 10 to 30 dB. The mean of OSNR estimation error M_{OSNR} is calculated by Eq. (10), and the standard deviation σ_{OSNR} is calculated by Eq.(11).

$$M_{OSNR} = \frac{1}{M} \sum_{j=1}^M (OSNR_{est,j} - OSNR_{ref,j}) \quad (10)$$

$$\sigma_{OSNR} = \sqrt{\frac{1}{M} \sum_{j=1}^M \left(OSNR_{est,j} - \frac{1}{M} \sum_{j=1}^M OSNR_{est,j} \right)^2} \quad (11)$$

where $OSNR_{est,j}$ is the estimated OSNR, and $OSNR_{ref,j}$ is the reference OSNR. As shown in Fig. 4(a), for each OSNR, the points of the error bars represent the maximum, mean, and minimum of the 20 OSNR measurements, and the black lines represent the reference OSNR.

To confirm the feasibility of the proposed OSNR monitoring method, we first measure the OSNR at B2B. The neighboring channels lasers are all turned off and the OSNR value is controlled by the Set OSNR module. From the Fig. 4, we can get that the $M_{OSNR} < 0.2$ dB, and the $\sigma_{OSNR} < 1.0$ dB at B2B, which proves that this method is feasible for measuring OSNR.

To further verify the anti-nonlinear performance of the OSNR monitoring method, we measure the OSNR after the signals transmit over a 1000 km optical fiber in five channels. The launch power is from 0 to 4 dBm for per channel, which will change the inter-channel NL. As show in Fig. 4, as the inter-channel NL interfere with the ASE noise power in the measurement zone, the estimation error increases with OSNR. When we keep other conditions fixed, increasing the OSNR means that the ASE noise power decreases. In this case, the effect of the inter-channel NL on the OSNR measurement will be relatively strengthened, resulting in an increase in the measurement error.

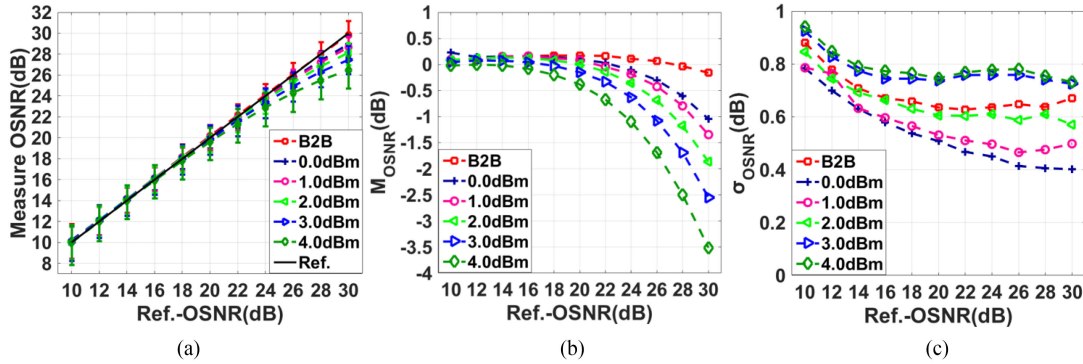


Fig. 4. Both at B2B and after five channel transmission over 1000 km with 0-4 dBm per channel launch power, (a) the maximum, mean, and minimum of the 20 OSNR measurements, (b) the mean of OSNR estimation error, and (c) the standard deviation of OSNR measurement.

In addition, with the increase of launch power, the NL effect in the fiber is enhanced, and more noise caused by NL covers the zone of our measurement, result in the estimation error increasing gradually. From Fig. 4(c), as the OSNR increases and the launch power decreases, the standard deviation of the measurement decreases. The M_{OSNR} is less than 1.0 dB with the OSNR range within 24 dB and the σ_{OSNR} is less than 1.0 dB. It proves that the proposed method has large NL tolerance to measure OSNR.

4. CD Monitoring Results

In order to measure CD, we first apply FrFT with different order on the received signal. Then we scan the orders by a step size of $\Delta p = 0.001$ to search for the optimum order. The mean of CD estimation error (M_{CD}) is calculated by Eq. (12), and the standard deviation (σ_{CD}) is calculated by Eq. (13).

$$M_{CD} = \frac{1}{M} \sum_{j=1}^M |CD_{est,j} - CD_{ref,j}| \quad (12)$$

$$\sigma_{CD} = \sqrt{\frac{1}{M} \sum_{j=1}^M \left(CD_{est,j} - \frac{1}{M} \sum_{j=1}^M CD_{est,j} \right)^2} \quad (13)$$

where $CD_{est,j}$ is the estimated CD, and $CD_{ref,j}$ is the reference CD.

To confirm the feasibility of the proposed CD monitoring method, we first measure the CD in single channel with OSNR = 14 dB. The signals transmit over the fiber with 100–2000 km to obtain the estimation error curve of the CD, as shown in Fig. 5. The M_{CD} is less than 80 ps/nm and the σ_{CD} is less than 80 ps/nm, demonstrating the feasibility of this method for monitoring CD. The $\sigma_{CD} = 0$ ps/nm means we can always search for the same optimal order under the corresponding conditions.

In order to research the anti-noise performance of the method for monitoring CD, we simulate the transmission distance of 5, 10, 15, 20 spans respectively in the case of single channel. The OSNR range is from 10 to 20 dB and the launch power is 0 dBm. The mean value of CD estimation error for different transmission distance with OSNR is shown in Fig. 6(a) and the standard deviation is shown in Fig. 6(b). As shown in Fig. 6(a), the M_{CD} is less than 90 ps/nm. The σ_{CD} is less than 95 ps/nm and decreases with increasing OSNR as shown in Fig. 6(b). These prove that this method has good anti-noise performance in CD monitor.

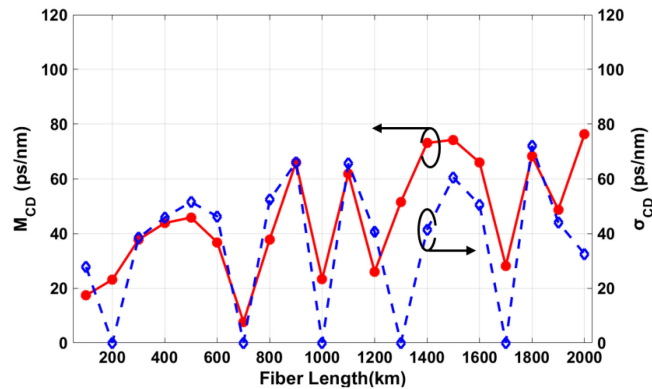


Fig. 5. CD estimation error for different accumulated CD from 1670 ps/nm to 34400 ps/nm when OSNR is 14 dB and without NL in single-channel link.

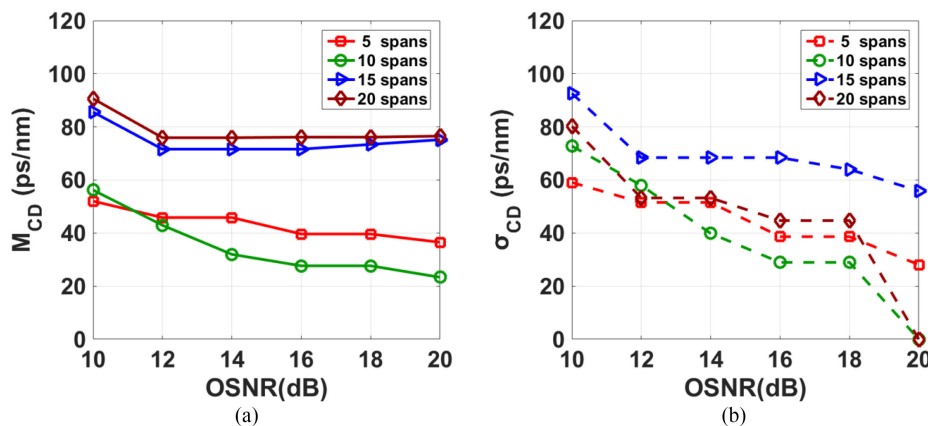


Fig. 6. The mean of CD estimation error (a) and the standard deviation (b) for 5, 10, 15, 20 spans with different OSNR (10–20 dB), and the number of channels is one.

Another factor affecting CD estimation error is the NL magnitude between channels. To explore the effect of NL on monitoring, we set up a 5 channels transmitting system. The middle channel transmits the QPSK-TS while the other 4 channels transmit standard QPSK signals. We control NL by changing the power of the signal. Here, we set the OSNR = 14 dB and simulate 5, 10, 15, 20 spans with the launch power is from 0 to 3 dBm, as showed in Fig. 7. It can be seen that the $M_{CD} < 90$ ps/nm and its change is small with both different launch power and different transmission distance, and the $\sigma_{CD} < 80$ ps/nm, which proves that the method has large NL tolerance.

5. Experimental Setup

To verify the proposed method with experiments, we set up a fiber optic link experimental platform as shown in Fig. 8. A laser with 5 kHz line width transmits into an I/Q modulator driven by a 20 Gbaud QPSK-TS signal source. The launch power of the signal is 0 dBm. The single-mode fiber has a length of 100 km, with dispersion coefficient 16.7 ps/nm, fiber loss 0.2 dB/km, and nonlinear coefficient 2.6×10^{-20} m²/W. By adjusting variable optical attenuator (VOA(b)) and VOA(c), the OSNR of the system is varied from 10 to 28 dB. The OSNR value measured in the optical spectrum analyzer (OSA) is used as reference value. After transmission, the signal is converted from the optical domain to the electrical domain after coherent reception and saved by digital storage oscilloscope

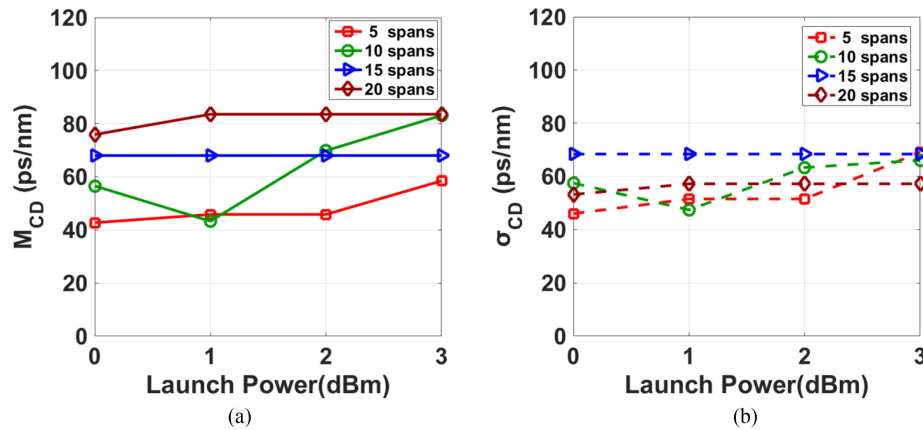


Fig. 7. The mean of CD estimation error (a) and the standard deviation (b) for 5, 10, 15, 20 spans with different launch power per channel (0–3 dBm), and the number of channels is 5.

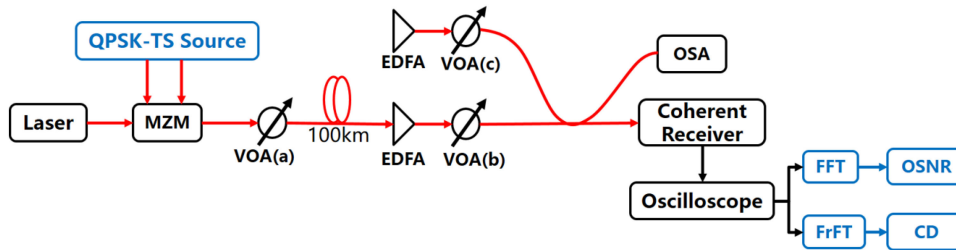


Fig. 8. Experiment setup of optic link transmission. VOA: variable optical attenuator. OSA: optical spectrum analyzer.

at 50 GSa/s. In the digital domain, the received signal is converted to the frequency domain by FFT for OSNR calculation, while it is converted to the fractional domain by FrFT for CD calculation.

6. Experimental Results

Due to the presence of ground noise in the experimental equipment, we first measure the power of this ground noise and obtain its frequency spectrum, which is used to correct the OSNR measurement. From the Eq. (2) and Eq. (3), the correction process can be expressed as:

$$P_{Total} = P_{Total-received} - P_{Total-ground} \quad (14)$$

$$N_{AM} = N_{AM-received} - N_{AM-ground} \quad (15)$$

where $P_{Total-received}$ is the total power of received signal, $P_{Total-ground}$ is the total power of ground noise, $N_{AM-received}$ is the power of noise in ASE measurement zone of received signal, $N_{AM-ground}$ is the power of noise in the same measurement zone as $N_{AM-received}$ but on the frequency spectrum of ground noise. The influence of ground noise on OSNR measurement can be reduced by this operation.

Based on the above proposed method, we measured the OSNR both at B2B and 100 km transmission conditions, respectively. The total number of the sampled data is 5000 for OSNR monitoring and we measure 100 times for each OSNR value to calculate its mean, maximum, minimum, and standard deviation as shown in Fig. 9. From Fig. 9 (a) and (b), it can be seen that as the reference OSNR increases, both M_{OSNR} and σ_{OSNR} are reduced first and then increased. This reflects the fact that in the experiment, when we change the OSNR by adjusting VOA(b) and

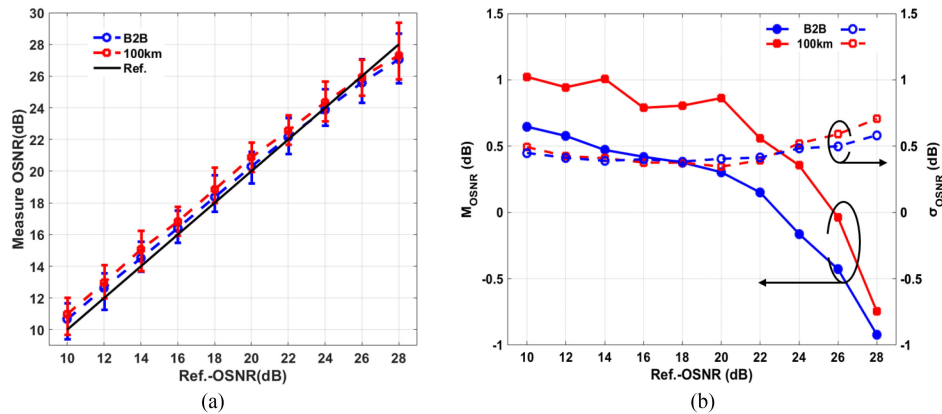


Fig. 9. Both at B2B and after single channel transmission over 100 km, (a) the maximum, mean, and minimum of the 100 OSNR measurements, and (b) OSNR mean estimation error and standard deviation.

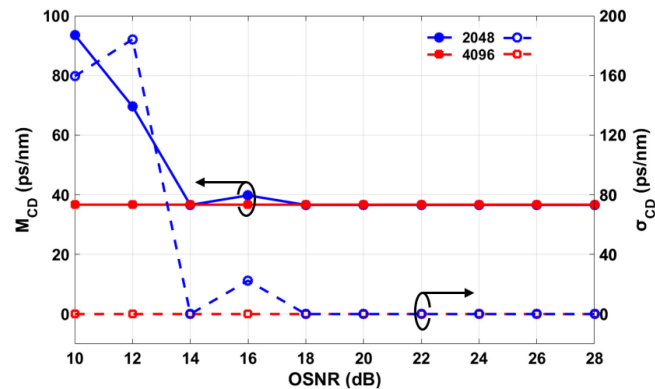


Fig. 10. The CD estimation error calculated by 2048 and 4096 samples after transmission over 100 km.

VOA(c), it is easy to cause overestimation when OSNR is small, and cause underestimation when OSNR is large. But both at B2B and 100 km transmission, the mean of OSNR estimation error is less than 1.0 dB and the standard deviation is less than 0.7 dB, which is acceptable.

In addition, 2048 samples and 4096 samples are used for calculating CD respectively, and we measure 100 times for each OSNR value to calculate its mean, maximum, and standard deviation. As shown in Fig. 10, increasing the number of samples will reduce the standard deviation of the result. When we use 4096 samples to calculate CD, the $M_{CD} < 40$ ps/nm and $\sigma_{CD} = 0$ ps/nm with the accumulated CD is 1670 ps/nm after 100 km transmission. This means that when searching for the optimal order of FrFT, we can always search for the same value, and the obtained CD measurement is also the same value, indicating that our method of measuring CD is stable and reliable. The above experimental results demonstrate the high accuracy in monitoring OSNR and CD, which proves that the proposed method is feasible and practical.

7. Conclusion

In this paper, we design a QPSK-TS for monitoring both OSNR and CD in DWDM systems. With the QPSK-TS design, it is allowed to calculate both OSNR and CD from the same set of data samples, which will reduce the sampling data types and save our sampling time. In the OSNR monitoring simulation, we measure the OSNR after the signals transmit over a 1000 km optical fiber in five

channels with the launch power is from 0 to 4 dBm for per channel. The M_{OSNR} is less than 1.0 dB with the OSNR range within 24 dB and the σ_{OSNR} is less than 1.0 dB, which proves that the proposed method has large NL tolerance to measure OSNR. In the CD monitoring simulation, we simulate the transmission distance of 5, 10, 15, 20 spans respectively with both the OSNR is from 10 to 20 dB in single channel and the launch power is from 0 to 3 dBm in five channels. The $M_{CD} < 90$ ps/nm and the $\sigma_{CD} < 95$ ps/nm, which proves that the method has good anti-noise performance and large NL tolerance in CD monitor. Furthermore, the experimental results demonstrate high accuracy of the proposed method (≤ 1.0 dB error within 28 dB and < 40 ps/nm error within 1670 ps/nm after 100 km single channel transmission). In the process of monitoring, communication services are not affected since there is no need to close any channel. Moreover, if we use the QPSK-TS as time domain pilot signal, the proposed method can be well applied to modern dynamically reconfigurable optical networks.

References

- [1] H. Y. Choi, J. H. Lee, S. K. Shin, and Y. C. Chung, "A review of the polarization-nulling technique for monitoring optical-signal-to-noise ratio in dynamic WDM networks," *J. Lightw. Technol.*, vol. 24, no. 11, pp. 4162–4171, Nov. 2006.
- [2] F. N. Hauske, M. Kuschnerov, B. Spinnler, and B. Lankl, "Optical performance monitoring in digital coherent receivers," *J. Lightw. Technol.*, vol. 27, no. 16, pp. 3623–3631, Aug. 2011.
- [3] S. Okamoto, F. Hamaoka, and Y. Kisaka, "Field trial of distance-adaptive optical transmission with digital in-band OSNR estimation," *Opt. Exp.*, vol. 24, pp. 22403–22412, 2016.
- [4] L. Dou, Z. Tao, Y. Zhao, and S. Oda, "Differential pilots aided in-band OSNR monitor with large nonlinear tolerance," in *Proc. Opt. Fiber Commun. Conf. Exhib.*, 2015, pp. 1–3.
- [5] L. Dou *et al.*, "An accurate nonlinear noise insensitive OSNR monitor," in *Proc. Opt. Fiber Commun. Conf. Exhib.*, 2016, pp. 1–3.
- [6] W. Wang, A. Yang, P. Guo, Y. Lu, and Y. Qiao, "Joint OSNR and inter-channel nonlinearity estimation method based on fractional Fourier transform," *J. Lightw. Technol.*, vol. 35, no. 20, pp. 4497–4506, Oct. 2017.
- [7] V. T. An *et al.*, "Chromatic dispersion estimation in 40 gb/s coherent polarization-multiplexed single carrier system using complementary golay sequences," in *Proc. Opt. Fiber Commun. Conf.*, 2012, pp. 1–3.
- [8] H. Zhou *et al.*, "Fractional Fourier transformation-based blind chromatic dispersion estimation for coherent optical communications," *J. Lightw. Technol.*, vol. 34, no. 10, pp. 2371–2380, May 2016.
- [9] F. N. Hauske, Y. Ye, I. T. Monroy, F. Pittala, and N. G. Gonzalez, "Combined CD and DGD monitoring based on data-aided channel estimation," in *Proc. Signal Process. Photon. Commun.*, 2011, pp. 1–2.
- [10] F. Pittal, F. N. Hauske, Y. Ye, N. G. Gonzalez, and I. T. Monroy, "Fast and robust CD and DGD estimation based on data-aided channel estimation," in *Proc. Int. Conf. Transparent Opt. Netw.*, 2011, pp. 1–4.
- [11] K. Ishihara, E. Yamazaki, T. Nakagawa, R. Kudo, T. Kobayashi, and Y. Miyamoto, "Fast chromatic dispersion estimation for coherent optical transmission systems," *Electron. Lett.*, vol. 48, no. 48, pp. 1290–1292, 2012.
- [12] W. Wang, Y. Qiao, A. Yang, and P. Guo, "A novel noise-insensitive chromatic dispersion estimation method based on fractional Fourier transform of LFM signals," *IEEE Photon. J.*, vol. 9, no. 1, Feb. 2017, Art. no. 7100312.
- [13] H. Zhou *et al.*, "A fast and robust blind chromatic dispersion estimation based on fractional Fourier transformation," in *Proc. Eur. Conf. Opt. Commun.*, 2015, pp. 1–3.
- [14] O. Akay and G. F. Boudreaux-Bartels, *Fractional Convolution and Correlation via Operator Methods and an Application to Detection of Linear FM Signals*. Piscataway, NJ, USA: IEEE Press, 2001.
- [15] V. A. Narayanan and K. M. M. Prabhu, "The fractional Fourier transform: Theory, implementation and error analysis," *Microprocessors. Microsyst.*, vol. 27, no. 10, pp. 511–521, 2003.
- [16] Y. Ma, P. Guo, and A. Yang, "A novel method for chromatic dispersion estimation with lower computation complexity in fractional domain," in *Proc. Int. Conf. Instrum. Technol.*, 2017, pp. 1–7.